Differential Capacitance of the Electrical Double Layer in Imidazolium-Based Ionic Liquids: Influence of Potential, Cation Size, and Temperature

ARTICLE *in* THE JOURNAL OF PHYSICAL CHEMISTRY C · APRIL 2008

Impact Factor: 4.77 · DOI: 10.1021/jp7100732

4 AUTHORS:

Vera N. Lockett
Nth Degree Technologies, Worldwide, USA
17 PUBLICATIONS **563** CITATIONS
SEE PROFILE

Rossen Sedev
University of South Australia
99 PUBLICATIONS **2,592** CITATIONS
SEE PROFILE

John Ralston
University of South Australia
332 PUBLICATIONS **10,009** CITATIONS
SEE PROFILE

Michael David Horne
The Commonwealth Scientific and Industrial…
38 PUBLICATIONS **1,159** CITATIONS
SEE PROFILE

THE JOURNAL OF PHYSICAL CHEMISTRY C

Article

Differential Capacitance of the Electrical Double Layer in Imidazolium-Based Ionic Liquids: Influence of Potential, Cation Size, and Temperature

Vera Lockett, Rossen Sedev, and John RalstonMike Horne, and Theo Rodopoulos

J. Phys. Chem. C, **2008**, 112 (19), 7486-7495 • DOI: 10.1021/jp7100732

Differential Capacitance of the Electrical Double Layer in Imidazolium-Based Ionic Liquids: Influence of Potential, Cation Size, and Temperature

Vera Lockett, Rossen Sedev,* and John Ralston

Ian Wark Research Institute, University of South Australia, Mawson Lakes, SA 5095, Australia

Mike Horne and Theo Rodopoulos

CSIRO Minerals, Box 312, Clayton South, VIC 3168, Australia

Received: October 17, 2007; In Final Form: December 17, 2007

The interfaces formed at glassy carbon electrodes in three low-temperature ionic liquids (1-methyl-3-ethylimidazolium chloride, emimCl; 1-methyl-3-butylimidazolium chloride, bmimCl; and 1-methyl-3-hexylimidazolium chloride, hmimCl) were investigated by cyclic voltammetry and impedance spectroscopy. The potential dependence of the differential double layer capacitance was measured at several temperatures between 80 and 140 °C, and the temperature response was found to be broadly similar to that obtained with high-temperature molten salts. The differential capacitance/potential curves have a minimum and two side branches. The minimum corresponds to the point of zero charge. The differential capacitance increases in the order hmimCl < bmimCl < emimCl because the double layer is thinner when imidazolium (Rmim) cations with shorter alkyl chain lengths are used. The impedance spectra and capacitance curves indicate that cations are adsorbed at the open-circuit potential and that their surface excess concentration increases with negative polarization. Adsorption of the cation becomes stronger as the length of the alkyl chain decreases. Adsorption of chloride anions occurs at positive potentials and is weakest with bmimCl. The increase in the differential capacitance with temperature is most probably due to ion association within the double layer, which diminishes as temperature increases. The electrochemical window narrows as the temperature increases but is almost unaffected by the length of the alkyl chain of the Rmim cation.

Introduction

Room-temperature ionic liquids (RTILs) are highly concentrated electrolytes.[1−7] Their properties vary over wide ranges, but the liquids that are most commonly used for electrochemical applications have wide electrochemical windows (up to 5−6 V[5]), have low volatilities, are nonflammable, are thermally stable (up to 250 °C), and have relatively low melting temperatures (below 100 °C). They have lower conductivities than all but dilute aqueous solutions at room temperature; however, this property is also a strong function of temperature.[8] It is clearly of practical and theoretical interest to study the temperature dependence of the double layer structure at an electrode immersed in an ionic liquid.

The use of ionic liquids in electrochemical capacitors is well-known.[9−11] The electrical double layer (EDL) capacitor is an energy storage device in which pseudoreversible electrochemical charge−discharge processes occur at the electrode/electrolyte interface.[12,13] Activated carbons are the most frequently used electrode materials because they have large specific surface areas. However, in EDL capacitors, it is also desirable to use electrolyte solutions that are stable over a wide range of potentials, and nonaqueous solvents such as alkyl carbonates and acetonitrile are common. More recently, RTILs have become popular for the same reason, and ionic liquids containing imidazolium cations, in particular, have been actively investigated in EDL capacitors.[9,14] Measurements of the potential dependence of the differential capacitance as a function of temperature provide critical information necessary for the design of EDL capacitors.

Ionic liquids have other important electrochemical applications: as electrolytes in lithium batteries, solar cells, and fuel cells; as solvents for the electrodeposition of metals, alloys, and semiconductors; and as solvents in the electrosynthesis of organics and polymers, for example.[5,7,15] Many of these applications depend on charge transfer across the electrode/electrolyte interface. The structure and properties of the EDL determine the rate and mechanism of the charge transfer and thus are key factors controlling the electrochemical reactions.

Despite the critical function played by the electrical double layer in these processes, there is little information about its structure and behavior at the conductor/ionic liquid interface. Theoretical studies of the EDL in ionic liquids are scant,[16,17] and efforts to determine EDL properties are also rare. The focus has been placed on measuring the differential double layer capacitance in ionic liquids at room temperature.[18−23] This lack of systematic experimental data severely limits development of a theory of the EDL at the conductor/ionic liquid interface.

The goal of the present work is the systematic investigation of the EDL properties of imidazolium-based ionic liquids. To this end, impedance spectroscopy and cyclic voltammetry were used over wide ranges of potential and temperature. The interfaces at glassy carbon electrodes immersed in three ionic liquids, namely, 1-methyl-3-ethylimidazolium chloride (emimCl), 1-methyl-3-butylimidazolium chloride (bmimCl), and 1-methyl-3-hexylimidazolium chloride (hmimCl), were investigated. This

* To whom correspondence should be addressed. E-mail: rossen.sedev@unisa.edu.au.

10.1021/jp7100732 CCC: $40.75
Published on Web 04/19/2008

strategy enabled the size of the cations to be varied without changing their overall physicochemical properties: all are 1-alkyl-3-methylimidazolium chlorides (RmimCl). The chloride anion was chosen as a common anion for all liquids because of its simple structure and known behavior at the solid electrode/electrolyte interface in aqueous solutions[24,25] and in molten salts.[26] To the best of our knowledge, these are the first determinations of the influence of cation size and temperature on the differential capacitance of the electrified solid/ionic liquid interface. (An article addressing similar phenomena has appeared[27] after this article was submitted for publication.)

Electrical Double Layer Capacitance of Molten Salts and Ionic Liquids

The thermodynamic definition of the differential capacitance of the double layer, C, for an ideally polarizable electrode (at constant temperature, T; pressure, P; and chemical composition, μ) is[28,29]

$$C = \left(\frac{\partial \sigma}{\partial E}\right)_{T,P,\mu} \tag{1}$$

where σ is the charge density on the electrode and E is the applied potential. The double layer capacitance is an experimentally measurable quantity, and its potential dependence is widely used in EDL investigations.

Numerous studies of the liquid metal/high-temperature ionic liquid interface have been conducted.[30] The potential dependence of the differential capacitance was found to have a parabolic shape, although the investigations of liquid metals in melts were limited to narrow potential ranges: less than 0.8 V.[26,31] These studies showed that the capacitance is much higher than in aqueous solutions and that it increases with temperature. Moreover, these studies determined that ion size influences the capacitance value and that the specific adsorption of the ions affects the shape of the differential capacitance/potential curve.[32] At inert solid electrodes, the capacitance curve exhibits several extrema.[33,34]

The simplest model of an electrified interface was suggested by Helmholtz.[35] The interface consists of two plates of opposite charge, as in a parallel-plate capacitor. The capacitance is given by[29,35]

$$C = \frac{\epsilon \epsilon_0}{d} \tag{2}$$

where ϵ is the dielectric constant of the material between the plates, ϵ_0 is the permittivity of free space, and d is the distance between the plates. Thus, as a first approximation, the double-layer capacitance depends on the thickness of the double layer and the dielectric constant of the electrolyte. Additional variables are considered in more sophisticated models.

The EDL theory for aqueous electrolytes is well-known, and elaborate models quantitatively describe the charge in the compact and diffuse layers, including differential and integral capacitances.[24,28,29,35] The experimental data for liquid metal/aqueous solution interfaces are described well, particularly for cases in which little specific adsorption occurs. However, one cannot apply this theory to molten salts or ionic liquids because there is no solvent; only anions and cations are present. As a consequence, when the EDL theory for aqueous solutions is applied to molten salts, it does not predict the capacitance increase with temperature or the high capacitance values (40 μF/cm^2 or more) at the minimum of the capacitance curve.

The EDL structure in a molten salt might be simpler than that in solutions because there are no solvent molecules; however, experimental measurements are complicated by the high temperature and the corrosiveness of the melt. It is also difficult to avoid the specific adsorption of ions in media where only ions are present. Theories have been developed to describe the double layer in molten salts, and equations have been derived to quantify the capacitance.[36−38] It has been suggested that the strong association between anions and cations in melts orders several layers of melt at the interface under the influence of the electric field. The expression derived for the charge distribution yields oscillations corresponding to a multilayer structure.[39] Sotnikov and Esin[37] assumed that, for any charge density in the metal, there is an equal and opposite charge density in the melt produced by vacancies. The theoretical results obtained with their model for the dependence of the differential capacitance on temperature and potential, derived without the use of adjustable parameters, were in reasonable agreement with experiments on cesium, rubidium, and potassium salts. However, their theory was applicable only for melts with similar anion and cation radii and for a liquid metal electrode.

The EDL structure and properties in molten salts were later described by other theories including the mean spherical approximation (MSA)[40,41] and the integral equation approximation.[42] However, none of these theories explains the increase in capacitance with temperature. The experimental differential capacitance/potential curves were not described in these studies because no distinction was made between differential and integral capacitance.

The increase with temperature of the capacitance at an uncharged interface was predicted by Monte Carlo simulations[43] for low reduced temperatures. Holovko et al.[44] suggested that the temperature increase of capacitance at relatively low temperatures (comparable to the melting points of molten salts) was related to a strong decrease in electrostatic interactions between the ions that led to ionic association. Supporting this suggestion, a Bjerrum-like correlation of the MSA was developed that was able to reproduce simulated data.[43]

Ionic liquids differ from molten salts in two critical ways: (i) the ions are generally large and frequently organic, and (ii) the upper limit of the thermal stability is not high enough to overcome the strong interionic interactions. Thus, even if Coulombic interactions were weak, internal structure in an ionic liquid might still form because of hydrogen-bonding, dipole−dipole, van der Waals, and hydrophobic interactions.[45] Yet despite these differences, room-temperature ionic liquids are highly concentrated electrolytes and are thus similar to high-temperature molten salts. Intuitively, one would therefore expect the capacitance behaviors of these two groups of materials to be broadly similar.

The available data for ionic liquids provide limited information about the influences of the anion and of the electrode material on the capacitance/potential curves. These curves exhibit complicated shapes.[18−23] The dependence of the double-layer differential capacitance as a function of the potential applied to a platinum electrode in bmim tetrafluoroborate and bmim dicyanamide was investigated.[18,19] The differential capacitance at the minimum of the curves was found to be 12 and 3.7 μF/cm^2, respectively. Nanjundiah et al.[21] investigated the EDL properties at a dropping mercury electrode in emim salts with various anions: $CF_3SO_3^-$ (triflate anion), $C(CF_3SO_2)_3^-$, $N(CF_3SO_2)_2^-$, and BF_4^-. They found the values of the EDL differential capacitance to be 10−15 μF/cm^2 at the potential of the minima. Double layer capacitance data for mercury in mixed

melts of $AlCl_3$ and 1-butylpyridinium chloride (bpyCl) have also been reported.[20] Different potential dependences were found for different $AlCl_3$/bpyCl ratios, but the minima of the differential capacitance/potential curves were distributed in a narrow interval centered at 20 μF/cm^2. The EDL capacitance without electrode polarization has been determined for various electrodes in contact with fused triethylammonium fluoroborate at 130 °C, using the impedance method.[23] The double layer capacitance was found to depend on the electrode material and to be on the order of 0.2−19 μF/cm^2.

In view of the lack of systematic data for well-characterized systems, we focused on glassy carbon electrodes in contact with a homologous series of imidazolium-based ionic liquids, as described below.

Materials and Methods

Great care was taken to purify all reagents used in the experiments, in order to minimize any possible contamination of the interface under investigation.

Ionic Liquid Purification and Analysis. Three types of impurities exert a strong influence on the properties of ionic liquids. Water, halide anions, and organic residues, left after synthesis, significantly affect properties such as viscosity, density,[46,47] electrochemical windows,[7,48,49] and others.[50] Water, in particular, narrows the potential window at both the cathodic and anodic limits.[5,49]

Three ionic liquids, namely, 1-methyl-3-ethylimidazolium chloride (emimCl, T_m = 83 °C), 1-methyl-3-butylimidazolium chloride (bmimCl, T_m = 60 °C), and 1-methyl-3-hexylimidazolium chloride (hmimCl, T_m = −85 °C), were obtained from Merck (purity grade for synthesis) and were thoroughly purified using the following procedure: Solid emimCl and bmimCl and liquid hmimCl were dissolved in water (Millipore, 18.5 MΩ cm), and extra-pure activated charcoal (Sigma-Aldrich) was added to the solutions to adsorb any organic impurities. The solutions were stirred for 48 h (at room temperature) and then filtered using 0.2-μm Teflon filters (Whatman). Remaining impurities were twice extracted from the filtrate into ethyl acetate (Chemsupply, HPLC grade), and solid emimCl and bmimCl were subsequently recrystallized from acetone (Chemsupply, HPLC grade). Residual solvents were finally removed under vacuum (0.1 mbar) and modest heating (70−80 °C). Just before an experiment was started, the ionic liquids were placed in the electrochemical cell used for the measurements and held at high vacuum and elevated temperature for 12−24 h to remove any residual water.

A Karl Fisher titrator (831 KF Coulometer, Metrohm) was used for water determinations. After 24 h at 100 °C and 5 × 10^{-5} mbar, the average water content of a sample was about 200 ppm. It is probable that some of this water had been absorbed by the highly hygroscopic liquids during the titration procedure.

All ionic liquids were characterized by NMR spectroscopy using a 200 MHz Varian NMR spectrometer, operating at 100 MHz for ^{1}H NMR spectroscopy and 50 MHz for ^{13}C NMR spectroscopy. No impurities were detected, and the results were in agreement with literature data.[51,52] For instance, the ^{1}H NMR spectrum (D_2O) of bmimCl consisted of the following peaks: δ 0.94 (t), 1.39 (sextet), 1.87 (q), 3.92 (s), 4.22 (t), 7.46 (s), 7.51 (s), 8.8 (s). The corresponding ^{13}C NMR spectrum included peaks at δ 15.41, 21.51, 33.99, 38.43, 52.05, 125.02, 126.29, and 138.57.

Working Electrode. Rod-shaped electrodes of glassy carbon (Sigradur G, Hochtemperature Werkstoffe GmbH) with a diameter of 1 mm were used in the experiments. The preparation of the working electrode surface is crucial for double layer investigations[53] and electrochemical experiments.[54,55] The results are affected not only by the microstructure and roughness of the electrode surface, but also by the blocking of active surface sites by adsorbed materials.

The electrode was polished using a BASi polishing kit and nylon pads. The surface was prepared using 15-, 3-, and 1-μm diamond paste and then 0.05-μm alumina powder to produce a mirrorlike finish. After each polishing step, the electrode surface was rinsed thoroughly with ethanol (after a diamond polish) or with water (after an alumina polish) and sonicated for 30 min. The glassy carbon electrodes were then annealed following a procedure described for Pt microelectrodes[56] that minimized oxidation. In this procedure, annealing was completed at 340 °C for 5 h under vacuum, and then the electrodes were cooled in a pure argon atmosphere. A droplet of ionic liquid was placed on the electrode working surface, and the electrode was transferred to the electrochemical cell, which was then evacuated.

The chemical composition of the electrode surface determined by X-ray photoelectron spectrometry showed a pure carbon surface with traces of oxygen (approximately 6%). Prior to capacitance measurements, the cleanliness of the electrode was further improved by cycling the potential within the limits of the electrochemical window.

For cyclic voltammetry and impedance experiments, the sides of the glassy carbon rod were protected from the ionic liquid in two ways. First, the sides were encapsulated in a modified Teflon heat-shrinkable tubing, leaving only the polished end of the electrode exposed. Second, a hanging electrolyte meniscus was always used. The rod was partially immersed in the ionic liquid and then withdrawn slowly until an upward meniscus was formed. The procedure was repeated at every operating temperature. Thus, the geometric area of the working electrode was well-defined and was calculated to be 0.785 mm^2.

It is important in these measurements to use the real surface area for polycrystalline metal or semiconductor electrodes.[57] To test whether the polishing procedure generated an acceptably smooth surface, a glassy carbon plate was polished and annealed following the same procedure. Its surface roughness was then assessed with an atomic force microscope (NanoScope III, DI). The scale of the roughness was found to be 1.6 nm over a scan area of 25 μm^2, and the ratio of real to projected surface area was 1.02. Consequently, the geometric area was used for all calculations in this work.

Reference and Counter Electrodes. A nonaqueous reference electrode of the second kind was used in the experiments. It was made of Ag|AgCl wire immersed in the liquid under investigation and separated from the bulk solution by a Vycor plug: Ag|AgCl|RmimCl (R = ethyl, butyl, or hexyl). The same ionic liquid used in the experiment was placed inside the reference electrode to eliminate the liquid junction potential. The reference electrode was always placed close to the working electrode, and *iR* compensation was performed automatically.

The platinum gauze counter electrode (4 cm^2, 100 mesh) had the shape of a hollow cylinder. Before every experiment, it was cleaned, annealed, and cooled in an inert atmosphere.

Electrochemical Cell. A jacketed, vacuum-tight cell was made from borosilicate glass. Two screw-thread vacuum fittings were used for the working and reference electrodes, which allowed the electrodes to be moved without compromising the vacuum during experiments. Cryptox fluoro-containing grease was used to seal the cell. All glass components of the

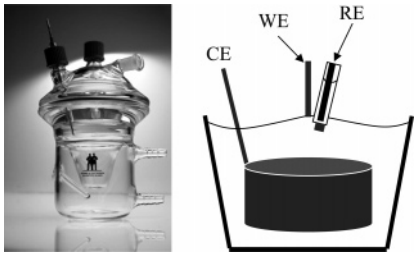

Figure 1. Electrochemical cell: WE, working electrode; CE, counter electrode; RE, reference electrode.

electrochemical cell were washed once with acetone, once with distilled water, and twice with boiling Millipore water (18.5 MΩ cm). The electrodes were placed as shown in Figure 1 with the face of the working electrode just touching the liquid at the center of the cell and the counter electrode arranged concentrically around it. The reference electrode was introduced from the side and positioned as close as possible to the face of the working electrode. A fixed volume (5 mL) of ionic liquid was used in every experiment.

The temperature was maintained with a HAAKE Phoenix II P1 circulator with an external Pt sensor (±0.01 °C) inserted inside the cell through a purpose-built tube (Figure 1).

Experimental Atmosphere. Ionic liquids are hygroscopic; hence, the experiments were carried out in a moisture-free atmosphere. Electrochemical experiments also require the exclusion of oxygen. Our experiments were conducted in high vacuum ($10^{-4}-10^{-5}$ mbar) or in ultrahigh-purity argon (99.999%) that contained no more than 1 ppm O_2 and 2 ppm H_2O.

Cyclic Voltammetry and Impedance Spectroscopy. The electrochemical investigations were carried out using a Zahner IM6-ex electrochemical workstation. Each experiment started with the recording several cyclic voltammograms, a procedure adopted for three reasons: (i) to clean the electrode surface before any measurement (from −1 to +1 V), (ii) to evaluate the potential range in which no reactions occur; and (iii) to confirm that the ionic liquid had not changed during the experiments. The scan rate was 10 mV/s throughout. Impedance measurements were carried out at different electrode potentials and temperatures using an ac signal of a 10 mV amplitude and a frequency range of $0.1-10^5$ Hz. Potentiodynamic measurements were made using a scan rate of 1 mV/s starting from the open-circuit potential. Data were fitted using the SIM software supplied with the Zahner workstation.

Rigorous electrode preparation and careful electrode design and arrangement inside the electrochemical cell were necessary to ensure that the impedance results were reliable. In particular, it is important that the area of the working electrode be much smaller than that of the counter electrode so that one can safely neglect the capacitance of the latter and attribute the total signal to the surface of interest. Also, the current distribution around the working electrode must be uniform.[55] The area of the counter electrode used in this study was over 500 times the area of the working electrode, so it is assumed that the above requirements were met.

Differential Capacitance Determination. *Electrical Properties of Glassy Carbon.* It is important that the electrical properties of glassy carbon not interfere with the capacitance measurements. Most importantly, the space-charge layer that forms at glassy carbon interfaces should not dominate the overall capacitance. In general, the measured differential capacitance at a semiconducting electrode will comprise contributions from the compact layer, the diffuse layer, and the space-charge layer.[58] The three capacitances are connected in series, and if low, the space-charge capacitance can dominate. Gerischer[58] estimated the density of states required for the space-charge layer to be restricted to a monolayer inside a semiconductor at 10^{22} cm^{-3} V^{-1}. The electrical properties of glassy carbon vary strongly with the heat-treatment temperature used during its synthesis. Sigradur G is a p-type semiconductor, synthesized at about 2000 °C, and has a band gap of about 0.035 eV.[59] A significant feature of the electronic structure of carbon is that, as disorder grows, a progressively greater number of localized states appear within the band gap.[60] Pesin and Baitinger developed a model to describe the unusual Seebeck (thermoelectric) effect in glassy carbon.[61] According to this model, the glassy carbon used in this study should have a density of "impurity" atoms that produce these localized states of 1.3×10^{22} cm^{-3}. Given the narrow band gap, this density of states should restrict the space-charge layer inside the glassy carbon to a monolayer. It is therefore not expected to interfere with the capacitance measurements carried out in this study. As an additional precaution, the capacitance measurements performed on glassy carbon were also repeated on gold and platinum electrodes in two different ionic liquids. The overall capacitance curves were influenced by the nature of RTIL and much less by the nature of the electrode material. This confirmed the insignificance of the space-charge capacitance.

Impedance Techniques. The differential capacitance ("capacitance" for short) and its dependence on potential (the "capacitance curve") can be obtained by impedance methods.

Within the electrochemical window of an unreactive electrolyte solution, glassy carbon is considered as an ideally polarizable electrode.[28,35,55] The total impedance of the cell then consists of the ohmic resistance of the electrolyte, *R*, and the double layer capacitance, *C*, in series. The impedance, *Z*, of the interfacial region between the working electrode and the reference electrode, at any dc potential, *E*, is given by the equation

$$Z = Z_{Re} + iZ_{Im} = R + (iC\omega)^{-1} \quad (3)$$

where *i* is the imaginary unit; Z_{Re} and Z_{Im} are the real and imaginary parts of the impedance, respectively; and ω is the angular frequency of the ac perturbation. Thus, at any electrode potential, the capacitance can be obtained from the measured impedance as

$$C = -(\omega Z_{Im})^{-1} \quad (4)$$

It is known, however, that polycrystalline and amorphous solid electrodes always show a capacitance dispersion with frequency.[62] The reasons for such dispersion have been discussed, and several concepts have been suggested. The first theories attributed it to the roughness of the electrode surface.[63] Atomic-scale defects (steps, kinks, dislocations) as well as microscopic roughness (corrugations, pits, grooves) are always present on the surface. These create inhomogenities in current density along the surface that entangle bulk solution resistance and interfacial capacitance, making it difficult to resolve the resistive and capacitive terms of the impedance.[63−65] Later, capacitance dispersion was attributed to the slow relaxation of the surface stress.[66] A modern view sees capacitance dispersion as interfacial in origin and caused by adsorption effects,[62,67] including slow formation of surface bonds or rearrangement of surface structures. It was experimentally demonstrated that roughness and adsorption effects are intrinsically coupled: an increased roughness broadens the time constant distribution of adsorption kinetics, thus increasing the capacitance dispersion.[62,67] In

practice, in order to reduce capacitance dispersion, it is necessary to make the metal electrode as smooth as possible and also to avoid conditions that promote specific adsorption.[62,67] This is difficult to achieve, as specific adsorption is quite prominent in many electrochemical systems.

The simplest way to treat nonideal capacitive behavior is to include in the model a constant phase element (CPE)[66−68] that has a power-law frequency dependence

$$Z_{\mathrm{CPE}} = Z_0(i\omega)^{-\alpha} = \frac{Z_0}{\omega^{\alpha}}\left(\cos\frac{\pi\alpha}{2} - i\sin\frac{\pi\alpha}{2}\right) \qquad (5)$$

where Z_0 and α are positive constants. Experiments performed on various solid metal electrodes have shown that the smoother and cleaner the surface and the lower the specific adsorption, the closer the value of α to unity, i.e., the closer the system to ideal capacitive behavior. For solid electrodes in aqueous solutions, α varies from 0.7 to 0.9.[62] Including nonideal capacitive behavior in eq 3 gives

$$Z = R + Z_0(i\omega)^{-\alpha} \qquad (6)$$

The capacitance can be obtained from the imaginary component of the impedance, Z_{Im}:

$$C = -(\omega Z_{\mathrm{Im}})^{-1} = \frac{\omega^{\alpha-1}}{Z_0\sin\frac{\pi}{2}\alpha} \qquad (7)$$

The capacitance curve can be determined accurately by either of following two methods. In the first one, impedance spectra are recorded at different potentials; then, every spectrum is fitted with eq 6, and the capacitance is calculated with eq 7. In the second approach, an appropriate frequency is found; then, a single-frequency impedance is measured at different potentials, and the capacitance is calculated via eq 4. The first approach is extremely slow and inconvenient experimentally. The electrode surface might be aging or gradually contaminated unless one records the spectra with large potential steps in order to save time. From this point of view, the second approach is preferable. However, it requires that the correct single frequency be determined before the experiments.

The capacitance curves in this work were obtained by the second method. However, the equivalence of the two methods was repeatedly cross-checked (using the full impedance spectra at various potentials in steps of 0.5 V) and was found to be satisfactory at 1 kHz. The anodic and cathodic limits for the potential scan were chosen to be 0.2−0.3 V inside the boundaries of the electrochemical window determined from cyclic voltammograms. Experiments were conducted at different temperatures in the range 80−140 °C. The direction of the temperature scan had no impact on the results. Measurements for each ionic liquid, including all preparation steps, were conducted in triplicate, and reproducibility of the results was good.

Results

If it is assumed that glassy carbon is an ideally polarizable electrode, then the capacitance can be calculated by the methods described in the previous section. Capacitance values, determined by the second method for glassy carbon in hmimCl over a range of frequencies (Figure 2), show that capacitance decreases with frequency. Thus, capacitance dispersion occurs on this electrode—as it does on many other solid electrodes—

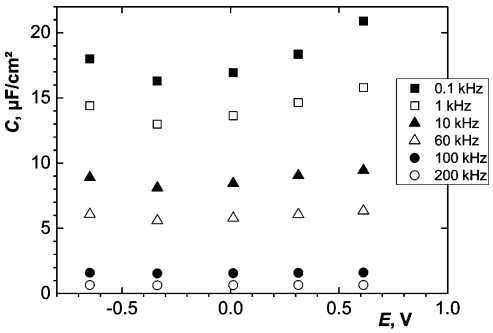

Figure 2. Differential capacitance curves obtained at different frequencies on a glassy carbon electrode in hmimCl at 100 °C. The potential was recorded against a Ag/AgCl/Cl$^-$ reference electrode.

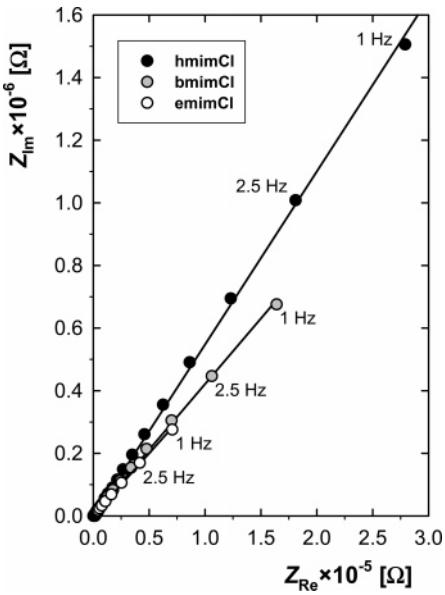

Figure 3. Nyquist plots of the impedance on glassy carbon in RmimCl at 120 °C and open-circuit potential. The lines are the best fits found using eq 6.

and one can use the more convenient second method only if a frequency is chosen such that the results are not distorted.

The impedance spectra for glassy carbon in the three ionic liquids at open-circuit potential (the equilibrium potential at which no net current flows to or from the electrode) are linear (Figure 3). Fitting based on eq 6, i.e., using a resistance and a CPE in series, describes the data collected between 1 Hz and 50 kHz very well. The lines have slopes of about 80°, and the fitting error for the capacitance in any ionic liquid did not exceed 3%. The values of α evaluated with the CPE scheme were 0.88 (hmimCl), 0.87 (bmimCl), and 0.85 (emimCl). The capacitance calculated from these measurements using eq 7 was approximately equal to the value obtained by the second method through eq 4 at a single frequency of 1 kHz (Figure 2). Thereafter, the impedance at different potentials was recorded at 1 kHz, the result was fitted with an equivalent circuit comprising a resistance and a capacitance in series, and the value of the capacitance was calculated using eq 4. The accuracy of the values obtained with this single-frequency method was cross-checked by measuring full impedance spectra at several potentials and using eq 6 to fit the data. The agreement was better than 0.5 μF/cm^2.

Care was taken to start these measurements from the open-circuit potential because the results were found to be irreproducible if measurements were started from other potentials. This is a common practice for molten salts[31,33] and aqueous systems[69]

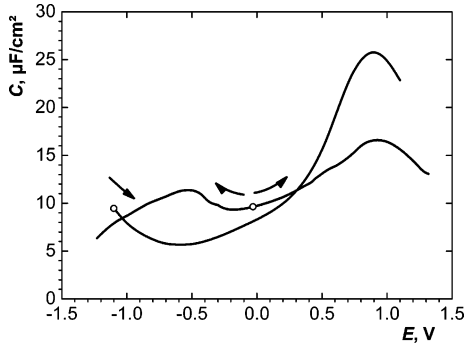

Figure 4. Differential capacitance for glassy carbon in hmimCl at 100 °C. Two scans are shown: one starting at the negative limit and scanning positively and one starting at the open-circuit potential and scanning first to one limit, waiting at the open-circuit potential for 30−40 min, and then scanning to the other limit.

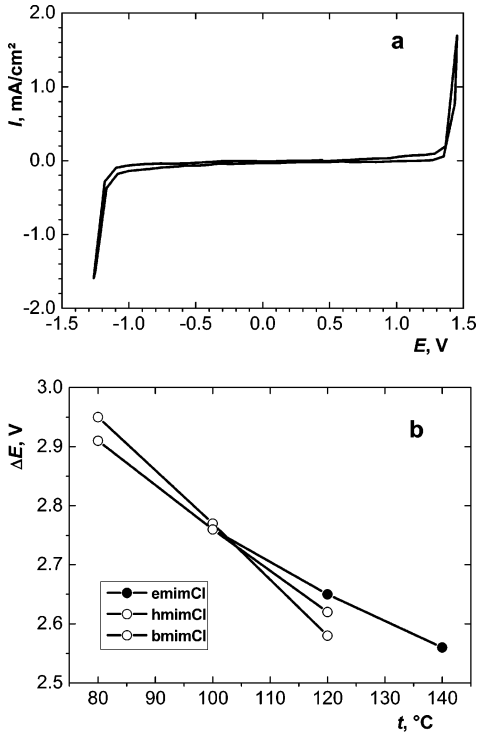

Figure 5. (a) Voltammogram for glassy carbon in emimCl at 120 °C. (b) Temperature dependence of the electrochemical windows.

for which irreproducibility of this type is seen. Figure 4 compares the differential capacitance values measured on glassy carbon in hmimCl at 100 °C using two different potential scans: one starting at the negative limit and scanning in the positive direction and the other starting at the open-circuit potential and scanning first to the one limit and then to the other, after a 30−40 min interval at the open-circuit potential. The difference in the results is clear, and only the second scan gives reproducible results. When the capacitance curves were recorded from negative to positive potential and back (curves not shown here), a considerable hysteresis was seen.

A typical voltammogram for glassy carbon immersed in emimCl at 120 °C is shown in Figure 5a. Within the potential range where the current density is small, the electrode is ideally polarizable, and any current is entirely due to EDL charging. The electrochemical window was determined using a cutoff current density of 1 mA/cm^2.[5] The electrochemical windows for the three ionic liquids (emimCl, bmimCl, and hmimCl) are similar and decrease linearly with temperature (see Figure 5b). The temperature coefficients are 5, 7, and 9 mV/K, respectively.

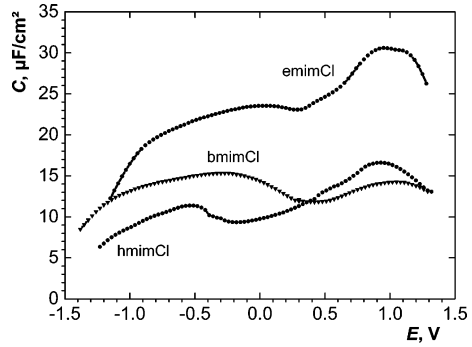

Figure 6. Differential capacitance curves for glassy carbon in RmimCl at 100 °C.

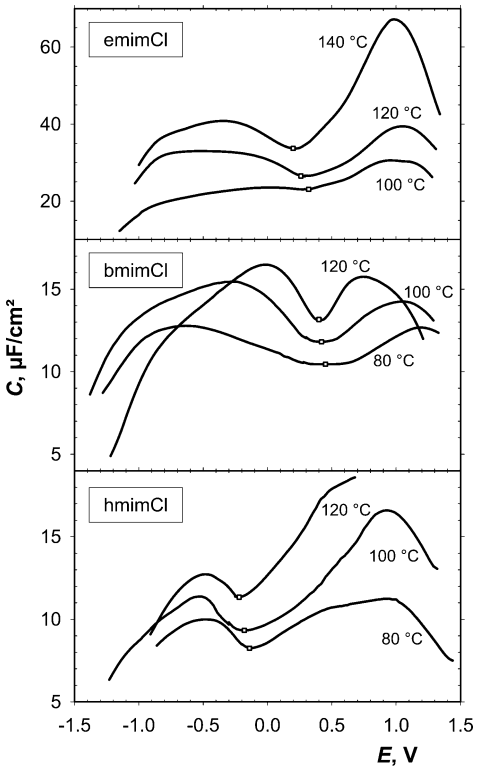

Figure 7. Differential capacitance curves for glassy carbon in RmimCl at different temperatures.

The capacitance curves for glassy carbon in the three ionic liquids at a single temperature (100 °C) are presented in Figure 6. The capacitance values decrease as the size of the cation (the length of its side alkyl chain) increases. The curves are broadly similar in shape and exhibit a minimum between two asymmetric maxima.

The influence of temperature on the capacitance curves obtained in all three ionic liquids is shown in Figure 7. In general, the capacitance values increase with temperature. The effect is more pronounced on the anodic side of the curve, and the minimum becomes steeper. Heating above 150 °C produced a dark coloration of the ionic liquids and a concurrent increase in current density, indicating that thermal degradation had begun.

Discussion

Electrochemical Windows. The electrochemical window of a system is of great practical significance. Its limits are set by the electrochemical reactivity of the system, and consequently, the redox reactions of the solvent are crucial. The electrochemical windows for glassy carbon in the ionic liquids investigated

here are approximately 2.5−3.0 V (Figure 5). This is wider than those found in aqueous solutions (~1.2 V) but relatively narrow compared to those of other ionic liquids because oxidation of the chloride anions establishes the positive limit. The negative limit of the electrochemical window is defined by reduction of the imidazolium ring. The width of the electrochemical window is virtually unaffected by the length of the alkyl chain of the imidazolium ring. A similar trend was found for $emimBF_4$ and $bmimBF_4$ on activated carbon, although in those systems, the window was 4.2 V.[10]

System without Polarization. When displayed as a Nyquist plot, the impedance spectra recorded without dc polarization (at the open-circuit potential) were straight lines that deviated systematically from the vertical (Figure 3). The deviation increased as the length of the alkyl chain of the imidazolium ring decreased. If, as has been proposed, adsorption lowers the parameter, then these results indicate that some adsorption occurs and increases on carbon in the order hmimCl ($\alpha = 0.89$) < bmimCl (0.88) < emimCl (0.86). Most likely, the cations adsorb preferentially because the open-circuit potentials are more negative than the local minima of the capacitance curves (Figure 6). Spectroscopic investigations in other systems have also shown that imidazolium-based cations adsorb at the electrode/electrolyte interface in the absence of polarization.[19,70−72]

System under Polarization. Nyquist plots of the impedance spectra at both positive and negative polarization deviated from straight lines at low frequencies (from 0.1 to 3−10 Hz), indicating that some slow processes occur. Because no charge transfer was detected by cyclic voltammetry, it is reasonable to suggest that these processes are related to adsorption or rearrangement of ions near the interface of the electrode. The impedance responses combined with observations of relaxation times in response to steps in the applied potential suggest that the time constants for these processes are between 10 ms and 1 s. By analogy with organic electrolytes dissolved in aqueous systems,[73,74] we suggest that these slow processes are related to the adsorption of the large and asymmetric Rmim cations. Note that hysteresis in the capacitance curves is typical of organic electrolytes adsorbed at surfaces from aqueous solutions, especially when the electrolytes contain long aliphatic chains or aromatic rings.

According to theories of the EDL in molten salts,[37,39] the ideal capacitance curve has a parabolic shape with a minimum at a potential known as the potential of zero charge (PZC). At the PZC, there is no excess charge on the metal or in the melt phase, and the positive (cationic) surface excess on the melt side of the interface equals the negative (anionic) surface excess.[55] The position of the capacitance minimum determined from impedance spectra and extrapolated to zero frequency corresponds closely to the PZC determined from electrocapillary curves.[75] The locations of the capacitance minima determined in this study did not vary with frequency (Figure 7) and were used as PZCs. (The values are listed in Table 1.)

The capacitance curves (Figure 6) are not parabolic, and their shape changes with temperature (Figure 7). However, care is needed when comparing capacitance curves from different systems because the potential windows over which the measurements were taken might not be wide enough for the comparison to be valid. For example, our curves have a parabolic shape in the potential range of 1.0−1.5 V, which is similar to that used for molten salts and aqueous solutions. Because we consider the minima as potentials of zero charge, the positive and negative branches of the curve correspond to the electrostatic attractions of anions and cations, respectively.

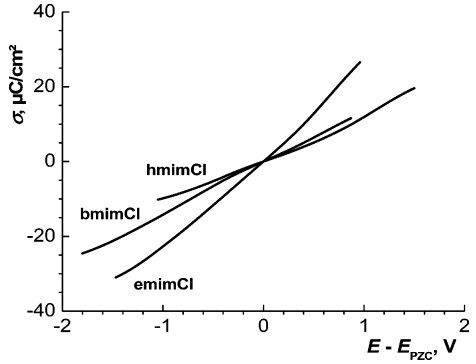

Figure 8. Charge density for glassy carbon in RmimCl at 100 °C.

TABLE 1: Potentials of Zero Charge, PZC, of the Glassy Carbon/Ionic Liquid Interface at Various Temperatures

ionic liquid	temperature (°C)	PZC[a]
emimCl	100	0.32
	120	0.26
	140	0.20
bmimCl	80	0.45
	100	0.42
	120	0.40
hmimCl	80	−0.14
	100	−0.18
	120	−0.22

[a] Values are in V, ±0.02 V, relative to a Ag|AgCl|Cl^- reference electrode.

Specific adsorption of ions at the electrified interface is also likely. Indeed, the deviation of the charge density/potential curves from linear relationships supports this assertion (Figure 8). These curves were calculated by integrating eq 1, and their potential dependences are steeper for smaller cations. It is well-known that Cl^- ions tend to be specifically adsorbed in both aqueous solutions[28,76] and molten salts,[31,32] and the same is true for large organic cations.[25] There is no solvent in our systems, and all contamination (e.g., surface-active species) was kept to a minimum. It therefore appears that the shape and magnitude of the negative and positive branches are influenced by specific ion adsorption.

Spectroscopic investigations of electrified interfaces provide unique information regarding chemical species adsorbed at the solid/liquid interface. For example, the structure of the gold/1-ethyl-3-methylimidazolium tetrafluoroborate interface has been investigated by in situ Fourier transform infrared reflection absorption spectroscopy.[70] In the potential range from −1.3 to +0.6 V (vs Ag|Ag^+), the emim cation was oriented close to the vertical, with either its methyl or ethyl group directed toward the gold surface. Surface-enhanced Raman scattering was used to probe the silver/1-butyl-3-methyl-imidazolium hexafluorophosphate interface.[71] The spectra showed that the bmim cation began to adsorb at −0.4 V (vs a Pt quasireference electrode) and the imidazolium ring was parallel to the surface at potentials more negative than −1 V. The orientation of the cation and anion at a platinum/1-butyl-3-methyl-imidazolium dicyanamide interface was investigated using sum frequency generation spectroscopy.[19] The spectra suggested that the imidazolium ring lies flat at the surface of the electrode at negative potentials. At more positive potentials, the anion seemed to be strongly adsorbed on the platinum surface, but interestingly, the cation did not leave the surface completely, preferring instead to adopt a tilted orientation (as a result of charge repulsion) to allow for anion adsorption. Similar cationic behavior was observed for Pt/$bmimPF_6$ and Pt/$bmimBF_4$.[72] The molecular orientation

TABLE 2: Capacitance at the PZC for Glassy Carbon/Ionic Liquid Interfaces at Different Temperatures[a]

ionic liquid	temperature (°C)	capacitance (μF/cm^2)
emimCl	100	23.1 ± 0.7
	120	26.5 ± 0.8
	140	33.7 ± 1.0
bmimCl	80	10.6 ± 0.3
	100	11.8 ± 0.4
	120	13.2 ± 0.4
hmimCl	80	8.2 ± 0.2
	100	9.3 ± 0.3
	120	11.3 ± 0.3

[a] Values refer to the geometric area of the electrode.

detected at solid surfaces is due to the strong solid−liquid interactions, and all of these studies concluded that specific adsorption was taking place.

The influence of the cation size on the adsorption of ions can be seen in Figure 6, where the negative branch corresponds to the adsorption of the Rmim cation. The shapes of these branches are nearly identical, indicating similar adsorption behaviors of all three cations with respect to polarization.

The positive branch corresponds to the adsorption of the chloride anion. The heights of these branches indicate that the adsorption of Cl^- is strongest for hmimCl and weakest for the bmimCl. It is known that larger cations facilitate the adsorption of anions because interactions between the ions are weaker, and in our case, it would seem that the longer alkyl chain of the hmim cation does not allow the anion to approach too closely. One can see this trend when comparing chloride adsorption for hmimCl and emimCl. However, bmimCl does not follow the trend, and the fact the temperatures studied are just above the melting point of this compound might be significant.

Capacitance at the PZC. There is a continuing discussion about the influence of cation size on the integral capacitance of carbon capacitors. It has been shown that, for phosphonium-based ionic liquids with a common anion, increasing the size of the cation decreases the overall capacitance of an activated carbon electrode.[77] This decrease in capacitance was suggested to be related to a decrease in the area of the porous carbon that is accessible to larger cations. In another study, the capacitance of activated carbon in emimBF_4 and bmimBF_4 was also found to decrease as the cation size increased.[10] Similar observations were made for high-temperature halide melts at a gold electrode.[31] The larger the alkali cation, the smaller the capacitance.

Our results clearly indicate that the double layer capacitance decreases as the size of the cation increases. The capacitance values at the PZC are listed in Table 2.

The capacitance strongly depends on the cation, whereas the electrochemical window is virtually unaffected—a very important consideration for the design of double layer capacitors.

From the capacitance minima, one can evaluate an effective thickness of the double layer, adopting the simple Helmholtz approach (eq 2). If one uses an approximate value for the permittivity of the ionic liquids ($\epsilon = 10$ [78,79]), the double layer thickness is 3.8 Å for emimCl, 7.5 Å for bmimCl, and 9.5 Å for hmimCl at 100 °C. These values are very close to the length of the major axis of the stretched Rmim cations, i.e., the double layer appears to be one ion thick.[18] There are two shortcomings with this interpretation. First, it implies that the cation is oriented perpendicularly to the electrode surface, whereas the real orientation of the imidazolium ring with respect to the interface remains a matter of debate. Second, the correspondence is good at 100 °C but significantly worse at 120 °C.

Temperature Dependence. Capacitance increases with temperature (Figure 7). This trend is also observed with high-temperature molten salts,[26,31,80] but as mentioned previously, there is no generally accepted explanation for this behavior. Sotnikov and Esin[37] relate it to the increased number of free vacancies in the melt with temperature. Another interpretation attributes the trend to the neglected frequency dependence of the measured capacitance in molten salts,[81] and yet another view suggests that the capacitance increase is linked to the accelerated dissociation of complex particles present within the double layer.[31] Theoretical models have been developed that suggest that this phenomenon results from decreased electrostatic interactions between the ions with increasing temperature.[44]

The change in shape of the capacitance curves with temperature in molten salts was considered to be a reversible reaction effect.[39] This explanation is not applicable for ionic liquids, because all of our measurements were taken in a potential range where current density did not exceed 1 μA/cm^2.

We propose that the growth and change in the capacitance/potential curves with temperature is likely to result from decreased ion association in the double layer with increasing temperature.[44] The presence of ion complexes in imidazolium-based ionic liquids was shown by time-of-flight secondary ion mass spectroscopy of the surface.[82] Measurements using dielectric spectroscopy also showed that about 8% of the ions in ionic liquids form contact ion pairs.[83] Thus, more ions are available for adsorption with increasing temperature, and they can get closer to the interface as a result of the breakdown of complexes present in the double layer. This behavior is amplified by weakening of the hydrogen bonding between the anion and hydrogen from the imidazolium ring with increasing temperature.

The rate at which the capacitance grows with temperature is different for different ionic liquids: bmimCl < hmimCl < emimCl (Table 2). Furthermore, the growth was found to accelerate with temperature. The acceleration was greatest for bmimCl. A similar tendency was found for molten salts where the temperature coefficient is larger for lithium and sodium halides than for potassium and cesium halides.[26,31]

Comparison with Theoretical Studies. Two significant theoretical studies of the electrical double layer in ionic liquids have recently appeared: one by Kornyshev,[16] who uses a mean-field gas-lattice model of the type previously used for concentrated electrolytes, and a second by Oldham,[17] who adopts a Gouy−Chapman−Stern approach and derives a similar outcome for the differential capacitance. The general shape of our capacitance curves is strikingly similar to that predicted by Kornyshev:[16] (i) the capacitance falls at potentials on either side of and far from the PZC, and (ii) the capacitance exhibits a local minimum at the PZC that results in a "camel-shaped" curve. We consider this similarity significant but caution against overstating it. Kornyshev explicitly states that his mean-field approach does not incorporate ionic correlations, fluctuations, or charge-density waves, nor does it take into account specific adsorption.[16] In this work, we have shown that specific adsorption occurs, and we have also hypothesized that the temperature effects are related to ion association.

Two key elements should be considered further. The first of these is the relative contributions of the compact and diffuse layers to the capacitance at potentials close to the PZC. According to Kornyshev the differential capacitance of the diffuse layer has a maximum near the PZC and decreases at large potentials.[16] Thus, only the second prediction matches the general shape of the capacitance curves presented here (Figure

7). However, close to the PZC, the capacitance of the compact layer becomes increasingly important and might well dominate the overall curve. We suggest that this is the reason for the minima that we observe experimentally. This speculation is qualitative, and clearly specific adsorption will have to be taken into account in the development of a quantitative prediction. The second element is the ion size asymmetry. For ionic liquids containing ions of nearly the same size, Kornyshev[16] derives a capacitance curve with a shape that varies with the parameter γ (the ratio of the total number of ions in the bulk to the total number of sites available to them). The curves are camel-shaped (rather than bell-shaped as in our case) only for $\gamma < 0.33$. Such a low value is improbable for RTILs, and therefore, the theory would predict bell-shaped curves when anions and cations are of similar sizes.[16] However, Kornyshev extended his consideration to include ions of different sizes (such as the RmimCl studied here). This extension, although semiempirical and speculative, leads to low values of γ and asymmetric camel-shaped capacitance curves for even modest differences in ion size.[16]

Conclusion

The differential capacitance values of a glassy carbon electrode in 1-methyl-3-ethylimidazolium chloride (emimCl), 1-methyl-3-butylimidazolium chloride (bmimCl), and 1-methyl-3-hexylimidazolium chloride (hmimCl) were obtained from impedance measurements. The shapes of the capacitance curves for the three ionic liquids are similar: a minimum and two side branches. The minimum corresponds to the point of zero charge. Capacitance grows in the order hmimCl < bmimCl < emimCl, as the double layer becomes denser for smaller imidazolium cations (shorter alkyl chain length). Both impedance spectra and capacitance curves indicate that some adsorption occurs. The shorter the alkyl chain of the Rmim cation, the stronger its adsorption. The adsorption of chloride anions is weakest in the case of bmimCl. The differential capacitance/potential curves can be explained using Kornyshev's mean-field theoretical considerations.[16] Capacitance increases with temperature, most probably as a result of weakening ion association. This behavior is broadly similar to that of high-temperature molten salts. The electrochemical windows shrink with temperature but are almost unaffected by the length of the Rmim alkyl chain.

Acknowledgment. Financial support from the Australian Research Council through its Special Research Centre Scheme and from CSIRO Minerals is gratefully acknowledged. Discussions with Dr. Bart Follink (CSIRO Minerals), Dr. Steve Feldberg (Brookhaven National Laboratories), and Prof. Leonid Pesin (Chelyabinsk State Pedagogical University) are warmly acknowledged.

References and Notes

(1) Rogers, R. D.; Seddon, K. R. *Science* **2003**, *302*, 792.
(2) Rogers, R. D.; Seddon, K. R. *Ionic Liquids as Green Solvents*; American Chemical Society: Washington, DC, 2003.
(3) Seddon, K. R.; Rogers, R. D. *Ionic Liquids III: Fundamentals, Progress, Challenges, and Opportunities*; American Chemical Society: Washington, DC, 2005; Vol. 901−902.
(4) Seddon, K. R.; Rogers, R. D. *Ionic Liquids: Industrial Applications for Green Chemistry*; American Chemical Society: Washington, DC, 2002.
(5) Ohno, H. *Electrochemical Aspects of Ionic Liquids*; Wiley: New York, 2005.
(6) Marsh, K. N.; Boxall, J. A.; Lichtenthaler, R. *Fluid Phase Equilib.* **2004**, *219*, 93.
(7) Buzzeo, M. C.; Evans, R. G.; Compton, R. G. *ChemPhysChem* **2004**, *5*, 1106.
(8) Galinski, M.; Lewandowski, A.; Stepniak, I. *Electrochim. Acta* **2006**, *51*, 5567.
(9) McEwen, A. B.; McDevitt, S. F.; Koch, V. R. *J. Electrochem. Soc.* **1997**, *144*, L84.
(10) Lewandowski, A.; Galinski, M. *J. Phys. Chem. Solids* **2003**, *65*, 281.
(11) Zhu, Q.; Song, Y.; Zhu, X.; Wang, X. *J. Electroanal. Chem.* **2006**, *601*, 229.
(12) Conway, B. E. *J. Electrochem. Soc.* **1991**, *138*, 1539.
(13) Vol'fkovich, Y. M.; Serdyuk, T. M. *Russ. J. Electrochem.* **2002**, *38*, 935.
(14) Yuyama, K.; Masuda, G.; Yoshida, H.; Sato, T. *J. Power Sources* **2006**, *162*, 1401.
(15) Endres, F. *ChemPhysChem* **2002**, *3*, 144.
(16) Kornyshev, A. A. *J. Phys. Chem. B* **2007**, *111*, 5545.
(17) Oldham, K. B. *J. Electroanal. Chem.* **2008**, *613*, 131.
(18) Baldelli, S. *J. Phys. Chem. B* **2005**, *109*, 13049.
(19) Aliaga, C.; Baldelli, S. *J. Phys. Chem. B* **2006**, *110*, 18481.
(20) Gale, R. J.; Osteryoung, R. A. *Electrochim. Acta* **1980**, *25*, 1527.
(21) Nanjundiah, C.; McDevitt, S. F.; Koch, V. R. *J. Electrochem. Soc.* **1997**, *144*, 3392.
(22) Galinski, M.; Kraewski, S. R. *Bulg. Chem. Commun.* **2006**, *38*, 192.
(23) Gatner, K. *Bull. Polish Acad. Sci. Chem.* **1984**, *32*, 379.
(24) Delahay, P. *Double Layer and Electrode Kinetics*; Interscience: New York, 1965.
(25) Bockris, J. O. M.; Khan, S. U. M. *Surface Electrochemistry: A Molecular Level Approach*; Plenum: New York, 1993.
(26) Ukshe, E. A.; Bukun, N. G.; Leikis, D. I.; Frumkin, A. N. *Electrochim. Acta* **1964**, *9*, 431.
(27) Alam, M. T.; Islam, M. M.; Okajima, T.; Ohsaka, T. *Electrochem. Commun.* **2007**, *9*, 2370.
(28) Grahame, D. C. *Chem. Rev.* **1947**, *41*, 441.
(29) Bockris, J. O. M.; Reddy, A. K. N.; Gamboa-Aldeco, M. *Modern Electrochemistry 2A. Fundamentals of Electrodics*, 2nd ed.; Plenum: New York, 2000; Vol. 2A.
(30) Inman, D.; Graves, A. D.; Sethi, R. S. Electrochemistry of Molten Salts. In *Electrochemistry*; The Chemical Society: London, 1970; Vol. 1, p 61.
(31) Dokashenko, S. I.; Stepanov, V. P. *Russ. J. Electrochem.* **1993**, *29*, 1297.
(32) Ukshe, E. A.; Bukun, N. G.; Leikis, D. I. *Bull. Acad. Sci. USSR Chem. Sci. [Engl. Transl.]* **1962**, *1*, 25.
(33) Graves, A. D.; Inman, D. *Nature* **1965**, *208*, 481.
(34) Tumanova, N. K.; Delimarskii, Y. K. *Electrochim. Acta* **1981**, *26*, 1737.
(35) Hunter, R. J. *Foundations of Colloid Science*; Clarendon Press: Oxford, U.K., 1987; Vol. 1.
(36) Dogonadze, R. R.; Chizmadzhev, Y. A. *Proc. Acad. Sci. USSR, Phys. Chem. [Engl. Transl.]* **1964**, *157*, 778.
(37) Sotnikov, A. I.; Esin, O. A. In *Physical Chemistry and Electrochemistry of Molten Salts and Slags (1966)*; Khimia: Leningrad, Soviet Union, 1968; p 209.
(38) Bukun, N. G.; Ukshe, E. A. In *Physical Chemistry and Electrochemistry of Molten Salts and Slags (1966)*; Khimia: Leningrad, Soviet Union, 1968; pp 214−23.
(39) Graves, A. D.; Inman, D. *Electroanal. Chem.* **1970**, *25*, 357.
(40) Blum, L. *J. Phys. Chem.* **1977**, *81*, 136.
(41) Painter, K. R.; Ballone, P.; Tosi, M. P.; Grout, P. J.; March, N. H. *Surf. Sci.* **1983**, *133*, 89.
(42) Booth, M. J.; Haymet, A. D. J. *Mol. Phys.* **2001**, *99*, 1817.
(43) Boda, D.; Henderson, D.; Chan, K.-Y. *J. Chem. Phys.* **1999**, *110*, 5346.
(44) Holovko, M.; Kapko, V.; Henderson, D.; Boda, D. *Chem. Phys. Lett.* **2001**, *341*, 363.
(45) Saha, S.; Hayashi, S.; Kobayashi, A.; Hamaguchi, H. *Chem. Lett.* **2003**, *32*, 740.
(46) Seddon, R. K.; Stark, A.; Torres, M.-J. *Pure Appl. Chem.* **2000**, *72*, 2275.
(47) Deetlefs, M.; Seddon, K. R.; Shara, M. *Phys. Chem. Chem. Phys.* **2006**, *8*, 642.
(48) Zhang, J.; Bond, A. M. *Analyst* **2005**, *130*, 1132.
(49) Schroder, U.; Wadhawan, J. D.; Compton, R. G.; Marken, F.; Suarez, P. A. Z.; Consorti, C. S.; Souza, R. F. d.; Dupont, J. *New J. Chem.* **2000**, *24*, 1009.
(50) Muldoon, M. J.; Gordon, C. M.; Dunkin, I. R. *J. Chem. Soc., Perkin Trans. 2* **2001**, *2*, 433.
(51) Huddleston, J. G.; Visser, A. E.; Reichert, W. M.; Willauer, H. D.; Broker, G. A.; Rogers, R. D. *Green Chem.* **2001**, *3*, 156.
(52) Zhou, Z.; Wang, T.; Xing, H. *Ind. Eng. Chem. Res.* **2006**, *45*, 525.
(53) Adamson, A. W.; Gast, A. P. *Physical Chemistry of Surfaces*, 6th ed.; Wiley: New York, 1997.

(54) Sawyer, D. T.; Sobcowiak, A.; Roberts, J. L. *Electrochemistry for Chemists*; Wiley: New York, 1995.
(55) Bard, A.; Faulkner, L. R. *Electrochemical Methods. Fundamentals and Applications*, 2nd ed.; Wiley: New York, 2001.
(56) Clavilier, J.; Faure, R.; Guinet, G.; Durand, R. *J. Electroanal. Chem.* **1980**, *107*, 205.
(57) Trasatti, S.; Petrii, O. A. *Pure Appl. Chem.* **1991**, *63*, 711.
(58) Gerischer, H. *Electrochim. Acta* **1990**, *35*, 1677.
(59) Jenkins, G. M.; Kawamura, K. *Polymeric Carbons: Carbon Fibre, Glass and Char*; Cambridge University Press: Cambridge, U.K., 1976.
(60) Thomas, J. M.; Evans, E. L.; Barber, M.; Swift, P. *Trans. Faraday Soc.* **1971**, *67*, 1875.
(61) Pesin, L. A.; Baitinger, E. M. *Carbon* **2002**, *40*, 295.
(62) Pajkossy, T. *J. Electroanal. Chem.* **1994**, *364*, 111.
(63) De Levie, R. *Electrochim. Acta* **1965**, *10*, 113.
(64) Borisova, T. I.; Ershler, B. V. *Zh. Fiz. Khim.* **1950**, *24*, 337.
(65) De Levie, R. *Electrochim. Acta* **1963**, *8*, 751.
(66) Lang, G.; Heusler, K. E. *J. Electroanal. Chem.* **1995**, *391*, 169.
(67) Pajkossy, T. *Solid State Ionics* **2005**, *176*, 1997.
(68) Brug, G. J.; Van den Eeden, A. L. G.; Sluyters-Rehbach, M.; Sluyters, J. H. *J. Electroanal. Chem.* **1984**, *176*, 275.
(69) Pajkossy, T.; Kolb, D. M. *Electrochim. Acta* **2001**, *46*, 3063.
(70) Nanbu, N.; Sasaki, Y.; Kitamura, F. *Electrochem. Commun.* **2003**, *5*, 383.
(71) Santos, V. O.; Alves, M. B.; Carvalho, M. S.; Suarez, P. A. Z.; Rubim, J. C. *J. Phys. Chem. B* **2006**, *110*, 20379.
(72) Rivera-Rubero, S.; Baldelli, S. *J. Phys. Chem. B* **2004**, *108*, 15133.
(73) Buess-Herman, C. Dynamics of adsorption and two-dimensional phase transitions at electrode surfaces. In *Adsorption of Molecules at Metal Electrodes*; Lipkowski, J., Ross, P. N., Eds.; VCH: New York, 1992; p 77.
(74) Lipkowski, J.; Stolberg, L. Molecular adsorption at gold and silver electrodes. In *Adsorption of Molecules at Metal Electrodes*; Lipkowski, J., Ross, P. N., Eds.; VCH: New York, 1992; p 171.
(75) Doubova, L. M.; Trasatti, S. *J. Electroanal. Chem.* **2003**, *550*−*551*, 33.
(76) Conway, B. E. *Solid State Ionics* **1997**, *94*, 165.
(77) Ania, C. O.; Pernak, J.; Stefaniak, F.; Raymundo-Pinero, E.; Beguin, F. *Carbon* **2006**, *44*, 3113.
(78) Wakai, C.; Oleinikova, A.; Ott, M.; Weingärtner, H. *J. Phys. Chem. B* **2005**, *109*, 17028.
(79) Bright, F. V.; Baker, G. A. *J. Phys. Chem. B* **2006**, *110*, 5822.
(80) Bukun, N. G.; Tkacheva, N. S.; Ukshe, E. A. *Sov. Electrochem.* **1970**, *6*, 1215−18.
(81) Kisza, A. *Electrochim. Acta* **2006**, *51*, 2315.
(82) Weingaertner, H.; Knocks, A.; Schrader, W.; Kaatze, U. *J. Phys. Chem. A* **2001**, *105*, 8646.
(83) Smith, E. F.; Rutten, F. J. M.; Villar-Garcia, I. J.; Briggs, D.; Licence, P. *Langmuir* **2006**, *22*, 9386.